10988 *Biochemistry* **2009,** *48,* 10988–10996
DOI: 10.1021/bi901427d

BIOCHEMISTRY
including biophysical chemistry & molecular biology
Article

The Platelet Receptor CLEC-2 Is Active as a Dimer[†]

Aleksandra A. Watson,[‡] Charita M. Christou,[‡] John R. James,[§] Angharad E. Fenton-May,[‡] Gerald E. Moncayo,[‡] Anita R. Mistry,[‡] Simon J. Davis,[∥] Robert J. C. Gilbert,[⊥] Aron Chakera,[‡] and Chris A. O'Callaghan*[,‡]

[‡]*Henry Wellcome Building for Molecular Physiology, University of Oxford, Roosevelt Drive, Oxford OX3 7BN, U.K.,* [§]*Howard Hughes Medical Institute, University of California, San Francisco, GH-N312E, MC 2200, 600 16th Street, San Francisco, California 94158-2517,* [∥]*Weatherall Institute of Molecular Medicine, John Radcliffe Hospital, Headington, University of Oxford, Oxford OX3 9DS, U.K., and* [⊥]*Division of Structural Biology, Henry Wellcome Building for Genomic Medicine, Roosevelt Drive, Oxford OX3 7BN, U.K.*

Received August 14, 2009; Revised Manuscript Received October 2, 2009

ABSTRACT: The platelet receptor CLEC-2 binds to the snake venom toxin rhodocytin and the tumor cell surface protein podoplanin. Binding of either of these ligands promotes phosphorylation of a single tyrosine residue in the YXXL motif in the intracellular domain of CLEC-2. Phosphorylation of this tyrosine initiates binding of spleen tyrosine kinase (Syk) and triggers further downstream signaling events and ultimately potent platelet activation and aggregation. However, it is unclear how a single YXXL motif can interact efficiently with Syk, which usually recognizes two tandem YXXL repeats presented as an immunoreceptor tyrosine-based activation motif (ITAM). Using bioluminescence resonance energy transfer, coimmunopreciptitation, recombinant protein expression and analytical gel filtration chromatography, surface plasmon resonance, Western blotting, multiangle light scattering (MALS), and analytical ultracentrifugation, we show that CLEC-2 exists as a non-disulfide-linked homodimer which could allow each Syk molecule to interact with two YXXL motifs, one from each CLEC-2 monomer.

Platelet activation and aggregation are of central importance in the primary hemostatic response which stops bleeding following vascular injury (*1*, *2*). Conversely, inappropriate platelet activation and aggregation can cause arterial thrombosis and occlusion, resulting in myocardial infarction, ischemic stroke, or other vascular diseases (*2*). Currently available antiplatelet therapy is of major benefit in preventing and treating these life-threatening diseases but is not without complications (*3*). A better understanding of platelet activation and how the molecules involved function is a key objective for biomedical research (*1*). CLEC-2 was identified through sequence similarity to C-type lectin-like immunoreceptors, such as NKG2D (*4*). The CLEC-2 gene is located in the human natural killer (NK)[1] complex on chromosome 12, which also encodes other similar molecules including the activating immune receptor NKG2D, the oxidized low-density lipoprotein receptor LOX-1, and the β-glucan receptor dectin-1 (*4*−*6*). CLEC-2 is a type 2 transmembrane receptor whose transcripts have been identified in bone marrow, liver, myeloid cells, and natural killer cells (*4*, *5*). CLEC-2 is expressed on platelets, and signaling through CLEC-2 is sufficient to trigger potent platelet aggregation (*7*, *8*). CLEC-2 on platelets is a receptor for the snake venom toxin rhodocytin, produced by the Malayan pit viper *Calloselasma rhodostoma* (*7*). We and others have shown that CLEC-2 is also a receptor for the transmembrane protein podoplanin, which has been implicated in tumor cell-induced platelet aggregation and tumor metastasis (*8*, *9*). We have solved the structures of CLEC-2 and rhodocytin, which are both C-type lectin-like molecules (*10*−*12*). The structure of podoplanin has not been determined, but the protein has no significant homology to rhodocytin nor any other structurally characterized protein. Sequence analysis indicates that it is a type 1 membrane protein with multiple O-linked glycosylation sites and a short cytoplasmic domain (*13*). Binding of rhodocytin or podoplanin to CLEC-2 leads to phosphorylation of the tyrosine residue in a single YXXL motif in the intracellular domain of CLEC-2 (*7*, *8*, *14*, *15*). Phosphorylation of this tyrosine promotes binding to the spleen tyrosine kinase (Syk) and triggers further downstream tyrosine phosphorylation events, PLCγ2 activation, and ultimately platelet aggregation (*7*, *15*). The ability of rhodocytin, podoplanin, or CLEC-2 specific antibodies to trigger platelet aggregation in the absence of other stimuli indicates the potency with which CLEC-2 can modulate platelet activity (*7*). Therefore, CLEC-2 is a potentially important therapeutic target in thrombotic cardiovascular disease (*13*).

Conventional immunoreceptor tyrosine-based activation motifs (ITAMs) contain two YXXL motifs within a larger consensus sequence, and the tyrosine residues in the ITAM can be phosphorylated by Src family kinases (*16*). Phosphorylation of these two tyrosine residues in the ITAM promotes binding to the ITAM by the tyrosine kinases Syk or Zap-70 via their tandem Src-homology 2 (SH2) domains, which leads to further downstream signaling (*16*−*18*). Although CLEC-2 interacts with Syk, this interaction is mediated by a single rather than dual YXXL motif within its cytoplasmic tail (*15*). It is currently unclear how a single YXXL motif can activate the Syk tyrosine kinase, which contains two tandem SH2 domains. In studies with truncated forms of Syk only two tandem Syk SH2 domains, and not a single Syk SH2 domain alone, were able to precipitate CLEC-2 from

[†]This work was funded by the Medical Research Council and British Heart Foundation. C.A.O'C. is an MRC Senior Clinical Research Fellow.
*To whom correspondence should be addressed. Tel: 44-1865-287789. Fax: 44-1865-287797. E-mail: chris.ocallaghan@ndm.ox.ac.uk.
[1]Abbreviations: BRET, bioluminescence resonance energy transfer; GFP, green fluorescent protein; MALS, multiangle light scattering; NK, natural killer; SH2, Src-homology 2; shRNA, small/short hairpin RNA; Syk, spleen tyrosine kinase; ITAM, immunoreceptor tyrosine-based activation motif.

 Published on Web 10/13/2009

stimulated platelets (*15*). In addition, site-directed mutagenesis of either individual SH2 domain in Syk abrogated CLEC-2 signaling (*15*, *18*−*20*). These results show that both Syk SH2 domains are required for productive CLEC-2 signaling, raising the possibility that Syk may bind to two CLEC-2 receptors simultaneously at the platelet surface.

Recombinant CLEC-2 expressed in bacteria is stable in solution as a monomer, and there is no suggestion of dimerization in the crystal structure and lattice packing (*10*, *12*). In addition, immunoprecipitation of CLEC-2 reportedly yields only a monomer (*7*). However, a number of other related C-type lectin-like receptors do form dimers (*21*−*25*). Close examination of the structure of CLEC-2 reveals a small hydrophobic surface patch at a site equivalent to the dimer interface in the scavenger receptor LOX-1, the immunoreceptors NKG2D and CD69, and the mouse Ly49 family of receptors (*10*, *21*−*25*). The site on CLEC-2 is smaller than the equivalent patch on related molecules but is distinct from the ligand binding area and could potentially play a role in dimerization. Here, we employ a range of techniques including bioluminescence resonance energy transfer, coimmunopreciptitation, recombinant protein expression and analytical gel filtration chromatography, surface plasmon resonance, Western blotting, multiangle light scattering (MALS), and analytical ultracentrifugation to determine the multimeric nature of CLEC-2 on the platelet surface and propose how CLEC-2 is capable of signaling through Syk, despite having only a single YXXL signaling motif.

EXPERIMENTAL PROCEDURES

Protein Expression and Purification. Constructs pOC189 and pOC550 encoding truncations of human CLEC-2 were expressed in *Escherichia coli* as inclusion bodies and refolded as previously described (*26*). The methods detailing the eukaryotic expression of glycosylated CLEC-2 protein from the pOC501 construct are described elsewhere (*8*). Refolded and nickel affinity purified proteins were analyzed and purified by gel filtration chromatography in 20 mM Tris, pH 8.0, and 150 mM NaCl with a Superdex 200 26/60 column on an AktaPurifier (GE Healthcare, Uppsala, Sweden). Rhodocytin was purified from the venom of *C. rhodostoma* as described previously (*11*, *27*, *28*). The purity and molecular weight of all samples were assessed by SDS−PAGE and mass spectrometry, respectively. Liquid chromatography electrospray ionization mass spectrometry was performed using a reverse-phase C4 column on an Ultima HPLC (Dionex, Sunnyvale, CA) connected to a quadrupole time-of-flight micromass spectrometer (Waters, Milford, MA). Recombinant podoplanin was made as described previously with a human IgG1 Fc region fused to its C-terminus (*8*).

Generation of Polyclonal Anti-CLEC-2 Sera in Mice. Four Balb/c mice were subcutaneously immunized with 50−100 μg of recombinant CLEC-2 pOC189 protein a total of four times. The antibody was validated by positive flow cytometry of cells transfected with CLEC-2 and negative flow cytometry on cells transfected with a range of related molecules.

Transfections. For coimmunoprecipitation, immunoblotting, and BRET experiments, HEK 293T cells were transiently transfected with plasmids encoding tagged or untagged full-length CLEC-2 using GeneJuice (EMD Novagen, Gibbstown, NJ) according to the manufacturer's instructions. Where indicated, a pSUPER RNAi mammalian expression vector (OligoEngine, Seattle, WA) containing a unique nucleotide sequence (AAGAUGGUUUGUCAACAGU) was used to specifically direct the intracellular synthesis of a small inhibitory hairpin RNA- (shRNA-) like transcript targeted against podoplanin. Jurkat cells were transfected using lipofectamine LTX supplemented with the PLUS reagent, according to the manufacturer's specifications (Invitrogen, Carlsbad, CA).

Immunoprecipitation and Immunoblotting. Cells were lyzed in 100 mM NaCl, 20 mM Tris, pH 7.5, 5 mM $MgCl_2$, and 0.5% Nonidet P-40 supplemented with Complete, EDTA-free protease inhibitor cocktail (Roche Applied Science, Basel, Switzerland). N-Terminally FLAG-tagged full-length CLEC-2 was immunoprecipitated for 24 h at 4 °C with anti-FLAG agarose affinity gel (Sigma, St. Louis, MO). Protein samples were boiled in reducing or nonreducing sample buffer, separated on 15% SDS−PAGE gels, and blotted onto nitrocellulose membranes, which were blocked in 5% (w/v) nonfat dried skimmed milk powder. Blots were then washed and incubated with either 10 μg of mouse anti-c-Myc monoclonal antibody (clone 9e10; Abcam, Cambridge, MA), mouse monoclonal anti-CLEC-2 antibody (R&D Systems, Minneapolis, MN), mouse monoclonal anti-GFP antibody (Roche Applied Science, Basel, Switzerland), anti-CLEC-2 polyclonal antibody obtained from mice immunized with recombinant CLEC-2 protein, or normal mouse serum. These membranes were then washed and incubated with horseradish peroxidase- (HRP-) conjugated goat anti-mouse immunoglobulin antibody and were subsequently visualized using 250 μM luminol, 405 μM *p*-coumaric acid, 0.1 M Tris, pH 8.5, and 0.05% H_2O_2.

Type 1 Bioluminescence Resonance Energy Transfer (BRET) Assay. GeneJuice (Novagen, Gibbstown, NJ) was used to transfect 60% confluent HEK 293T cells, with varying ratios of plasmids encoding full-length human CLEC-2 protein, tagged at its cytoplasmic N-terminus with either GFP2 or luciferase. Cells were harvested 48 h posttransfection, and for each transfection, 10 μM DeepBlueC coelenterazine (Perkin-Elmer, Waltham, MA) was added to 100 μL of cells in a 96-well plate, and light emission in the 410 ± 40 and 515 ± 15 nm wavelength ranges was collected immediately as described elsewhere (*29*). GFP2 and luciferase expression were measured in separate wells and converted to a ratio of concentrations (*29*).

Confocal Microscopy. Forty-eight hours posttransfection, cells were attached to coverslips, excited with an argon 488 nm laser, and examined using a Zeiss LSM510 confocal microscope under an oil immersed objective, according to the manufacturer's instructions (Carl Zeiss MicroImaging, Munich, Germany).

Flow Cytometry. Cells were washed in cold phosphate-buffered saline containing 0.5% FCS and incubated for 20 min at 4 °C with either phycoerythrin- (PE-) labeled tetrameric recombinant CLEC-2 protein, monoclonal anti-CLEC-2 antibody (R&D Systems, Minneapolis, MN), rat monoclonal anti-(human podoplanin) antibody NZ-1 (AngioBio, Del Mar, CA), or the appropriate isotype control (*8*). Cells were washed and then incubated with a phycoerythrin-conjugated anti-mouse or anti-rat IgG secondary antibody for 20 min on ice and then washed further before immediate acquisition on a FACS Canto flow cytometer (Becton-Dickinson, Franklin Lakes, NJ). Data were analyzed using FlowJo software (Tree Star, Ashland, OR).

Surface Plasmon Resonance. Equilibrium experiments were performed as described previously (*8*, *10*, *30*). Briefly, binding studies were conducted using a Biacore T100 (GE Healthcare, Uppsala, Sweden) instrument. Protein A was attached to carboxymethylated dextran-coated CM5 sensor chips

using amine coupling. Recombinant podoplanin Fc fusion protein and an irrelevant control Fc fusion protein, CD44, were each immobilized at equivalent levels on two pairs of these protein A-coated surfaces. The arrangement was such that each experimental flow cell coated with podoplanin (typically around 150−200 response units or 600−800 response units) was compared to a reference control flow cell coated with an equivalent amount of control protein. Recombinant CLEC-2 protein expressed from either construct pOC550 or pOC501 was injected over the surfaces, and experiments were performed in 10 mM HEPES, pH 7.4, 150 mM NaCl, 3 mM EDTA, and 0.005% polysorbate 20 (v/v). K_d values were obtained by nonlinear curve fitting of the 1:1 Langmuir binding isotherm (bound = $C \times \max/(K_d + C)$, where C is analyte concentration and max is the maximum analyte binding) to the data using the Levenberg−Marquardt algorithm as implemented in the program Origin (OriginLab Corp., Northampton, MA). Global fitting was used, and the error computed is the standard error of the fit from a global analysis of all the data.

Dynamite Computational Dynamic Analyses. As we have previously described, a model of the three-dimensional structure of dimeric human CLEC-2 was assembled manually by superimposing two copies of the monomeric CLEC-2 structure (2C6U) onto the dimeric structure of the oxidized low-density lipoprotein receptor LOX-1 (1YPQ), the most closely related dimeric C-type lectin-like structure, using Coot (*11*, *31*). This dimeric CLEC-2 model was regularized and prepared for Dynamite computational dynamic analyses using energy minimization algorithms implemented by the Whatif server (*32*). Model dimeric CLEC-2 was further refined using energy minimization algorithms implemented by CNS solve (*10*, *33*). The Dynamite package was used to infer, analyze, and graphically represent the likely modes of motion of monomeric and dimeric CLEC-2 (*34*). The graphical representations of the dynamic analyses were visualized with VMD (*34*, *35*).

Multiangle Light Scattering (*MALS*). MALS experiments were performed using an analytical Superdex 75 10/30 column (GE Heathcare, Uppsala, Sweden) with online static light scattering (Dawn Heleos II; Wyatt Technology, Santa Barbara, CA), differential refractive index (Optilab rEX; Wyatt Technology), and Agilent 1200 UV (Agilent Technologies, Santa Clara, CA) detectors. Proteins used for MALS were concentrated to 20 μM. Data were analyzed using the ASTRA software package (Wyatt Technology).

Mass Spectrometry. Liquid chromatography electrospray ionization mass spectrometry was performed using a reverse-phase C4 column on an Ultima HPLC (Dionex, Sunnyvale, CA) connected to a quadrupole time-of-flight micromass spectrometer (Waters, Milford, MA).

Analytical Ultracentrifugation. Sedimentation equilibrium analytical ultracentrifugation experiments were performed in a Beckman XL-I analytical ultracentrifuge. Samples were loaded in an An60Ti rotor with an equilibrium six-channel centerpiece (path length 1.2 cm) and run at 11000, 14000, and 19000 rpm, at 20 °C. Interference and absorbance data were both collected, with the latter obtained at wavelengths of 254, 280, and 305 nm. Scans were taken after 12 and 14 h at each rotor speed. Analysis of the data, including estimation of average molecular mass, was carried out using UltraSpin2 software developed by Dmitry Veprintsev (ultraspin.mrc-cpe.cam.ac.uk), and curve fitting was performed using Origin (OriginLab Corp., Northampton, MA). The data were analyzed using two partial specific volumes for the glycosylated protein pOC501, 0.6970 and 0.7100 cm^3/g, determined from protein sequence and accounting for the minimum and maximum levels of protein glycosylation, respectively, as determined by mass spectrometry.

RESULTS

Glycosylated Recombinant CLEC-2 Protein Forms a Stable Dimer. Recombinant CLEC-2 protein encoding the C-terminal C-type lectin-like domain and refolded from inclusion bodies produced in *E. coli* was homogeneous and pure and is exclusively monomeric and binds both of its ligands, rhodocytin and podoplanin (*8*, *10*). The crystal structure and lattice packing of this CLEC-2 protein do not indicate any higher order oligomerization (*10*). However, this recombinant protein contains only residues 96−221 of CLEC-2 and so lacks a putative stalk region N-terminal to the C-type lectin-like domain (*26*). A construct (pOC550) was, therefore, designed to include this stalk sequence in addition to the C-type lectin-like domain and was expressed in *E. coli* as inclusion bodies, refolded, and purified by gel filtration (Figure 1A). This protein eluted from a Superdex 200 26/60 gel filtration column as both a dimer and a monomer, in contrast to the crystallized protein, which elutes in a single peak corresponding to the molecular mass of monomeric CLEC-2 protein (Figure 1B,C). This suggests a possible role for the stalk region of CLEC-2 in facilitating homodimerization. To exclude artifacts relating to the refolding process, a construct (pOC501) containing the same sequence and incorporating the stalk region was expressed in HEK 293T cells. This protein, although similar in terms of sequence to the bacterial construct pOC550, purified exclusively as a dimer (Figure 1D). Size exclusion chromatography with online multiangle laser light scattering (MALS) of this eukaryotic CLEC-2 protein confirmed that this protein is of the approximate molecular mass corresponding to a dimer. Analytical ultracentrifugation equilibrium sedimentation experiments further verify that CLEC-2 protein encoded by plasmid pOC501 exists as a dimer (Figure 1E,F). Mass spectrometry of this glycosylated protein revealed a molecular mass ranging from 31132 to 39370 Da. This heterogeneity is predominantly caused by varying degrees of glycosylation as we have previously shown that this protein has around 13 kDa of glycosylation per monomer (*8*). Interference (Figure 1E) and absorbance (Figure 1F) data were analyzed using two partial specific volumes to represent the minimum and maximum levels of glycosylation as determined by mass spectrometry. Based on the minimal and maximal levels of glycosylation, the molecular masses at infinite dilution were calculated from the absorbance data to be 60244 ± 681 and 62093 ± 1144 Da, respectively. Using the interference data, these values were determined to be 65396 ± 2150 and 68423 ± 2268 Da. These data demonstrate that CLEC-2 is dimeric in solution. The refolded CLEC-2 protein pOC550 was also analyzed by mass spectrometry and has a mass of 18387 kDa, consistent with the presence of four disulfide bonds in each monomeric subunit, three of which reside in the C-type lectin-like domain, as observed in the crystal structure of CLEC-2, and a further one which must be between cysteines 81 and 99 within the stalk portion. Protein expressed from the bacterial expression plasmid pOC550 is prone to aggregation following purification by gel filtration, but CLEC-2 protein generated from pOC189 is stable in solution under these conditions, indicating that the addition of the stalk segment of CLEC-2 in the absence of protein glycosylation reduces the solubility of the bacterially expressed protein. These observations suggest that

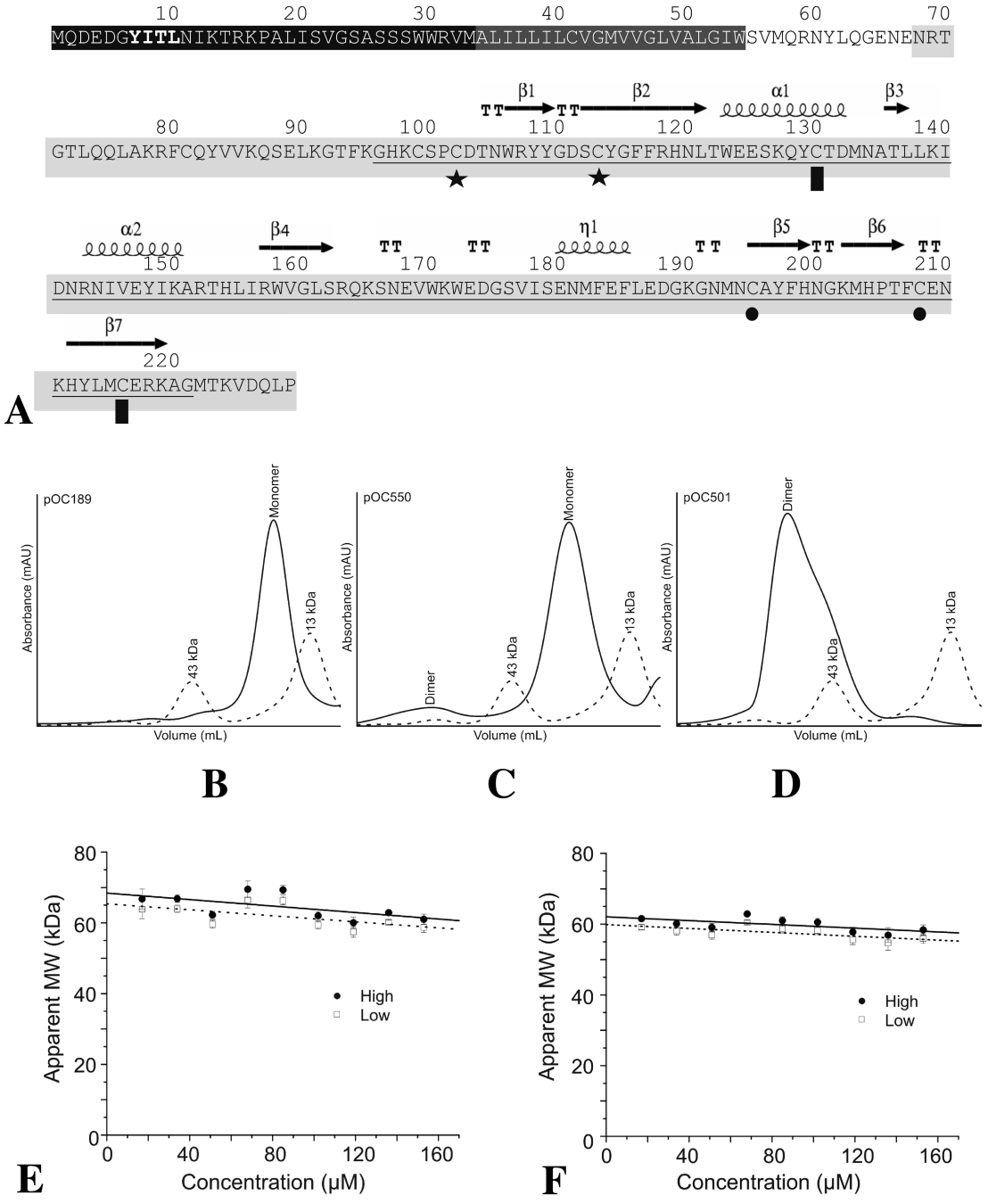

FIGURE 1: Recombinant CLEC-2 is stable both as a monomer and as a dimer. (A) The full-length protein sequence of human CLEC-2 is represented. The predicted intracellular and transmembrane portions are highlighted in black and dark gray, respectively. The recombinant proteins that included the putative stalk region (encoded by pOC501 and pOC550) are highlighted in light gray, and the shorter construct pOC189 which was crystallized is underlined. The cytoplasmic YXXL motif is marked in bold text. Predicted paired cysteines are marked with matching black symbols (stars, circles, or rectangles) beneath the text. The secondary structural elements of CLEC-2 are indicated above the text. (B−D) Black traces represent size exclusion gel filtration chromatograms for recombinant refolded CLEC-2 protein expressed in bacteria from plasmids pOC189 (B) and pOC550 (C) and recombinant CLEC-2 protein expressed from the plasmid pOC501 in HEK 293T cells (D). Size standards are shown for comparison (dotted lines). (E, F) The molecular mass of protein expressed from plasmid pOC501 in eukaryotic cells was determined by sedimentation equilibrium analytical ultracentrifugation. Protein concentration (μM) is plotted against molecular mass (kDa) as calculated from interference (E) and absorbance (F) data using the partial specific volume based on the lower (empty squares) and upper (black circles) limits of the range of glycosylation as determined by mass spectrometry.

CLEC-2 protein that includes the stalk region is stabilized by glycosylation.

CLEC-2 Is Active As a Dimer. To assess whether dimeric CLEC-2 is functional, we performed surface plasmon resonance experiments. Using dimeric recombinant CLEC-2 expressed from bacterial expression plasmid pOC550, we were able to demonstrate unambiguous binding to recombinant podoplanin but not to an irrelevant control protein made using the same expression system (Figure 2). The estimated affinity of the interaction (4.1 ± 0.2 μM) is approximately 6 times higher than that of the recombinant monomeric protein (*8*). Dimeric CLEC-2 protein expressed in HEK 293T cells from construct pOC501 also bound specifically to podoplanin as demonstrated by surface plasmon resonance binding assays (data not shown). These binding studies confirm that dimeric CLEC-2 is functional and has a higher

affinity for the endogenous ligand podoplanin than monomeric protein.

CLEC-2 Forms Membrane-Bound Homodimers. To investigate whether membrane-bound CLEC-2 forms homodimers, we performed immunoprecipitations. Plasmid constructs encoding full-length human CLEC-2 coupled to either a c-Myc or FLAG tag at its cytosolic N-terminus were cotransfected into HEK 293T cells. Cell lysates were immunoprecipitated with an anti-FLAG monoclonal antibody and then Western blotted with an anti-c-Myc monoclonal antibody. Anti-c-Myc blotting detected a band that was coimmunoprecipated with FLAG-tagged CLEC-2 and which corresponded in size to c-Myc-tagged CLEC-2 (Figure 3A). This demonstrates a strong association between the two tagged forms of CLEC-2 and indicates that full-length CLEC-2 forms dimers or higher order multimers at the cell surface.

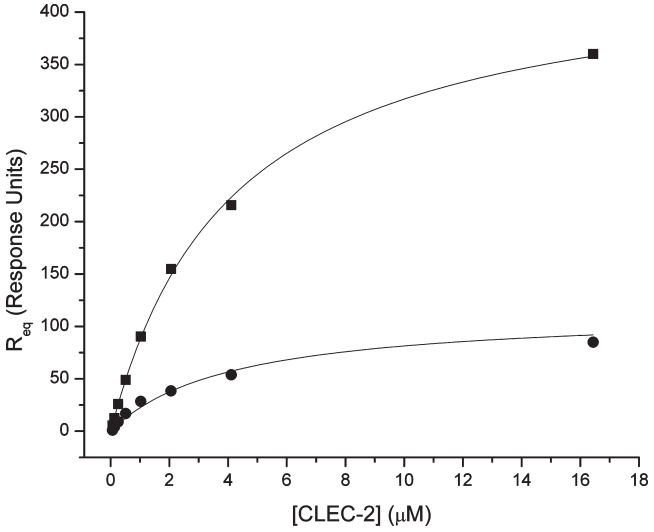

FIGURE 2: Dimeric CLEC-2 is functional and binds podoplanin. The surface plasmon resonance equilibrium binding response is plotted as a function of CLEC-2 concentration. CLEC-2 was flowed over surfaces coated with podoplanin or control protein. The curves represent the best fit to the experimental data using global fitting. The two sets of points (squares and circles) are taken from different flow cells on the same chip, both coated with different amounts of podoplanin and referenced by subtraction of the signal from control flow cells coated with equivalent amounts of control protein.

We have shown that podoplanin is an endogenous ligand for CLEC-2 and that podoplanin is expressed in HEK 293T cells (*8*, *9*). To determine whether CLEC-2 oligomerization in these cells was caused by ligand-induced self-association of CLEC-2 molecules, we used RNAi to reduce podoplanin expression. The small inhibitory RNA-like transcript used has previously been shown to knock down the surface expression of podoplanin (*36*). The shRNA-generating plasmid DNA was cotransfected with the FLAG- and c-Myc-tagged CLEC-2 constructs into HEK 293T cells, and coimmunoprecipitations were performed as above. Reduction of podoplanin in transfected cells was confirmed by flow cytometry using an anti-podoplanin antibody (Figure 3B). Western blot analysis revealed that, despite the shRNA-mediated lowering of podoplanin expression, c-Myc-tagged CLEC-2 was still detected at equivalent levels in cell lysates which had been immunoprecipitated with anti-FLAG resin (Figure 3A). To confirm that podoplanin was not influencing these results, the coimmunoprecipitations were repeated in the Jurkat T-cell line. Jurkat cells do not express podoplanin and or any other putative

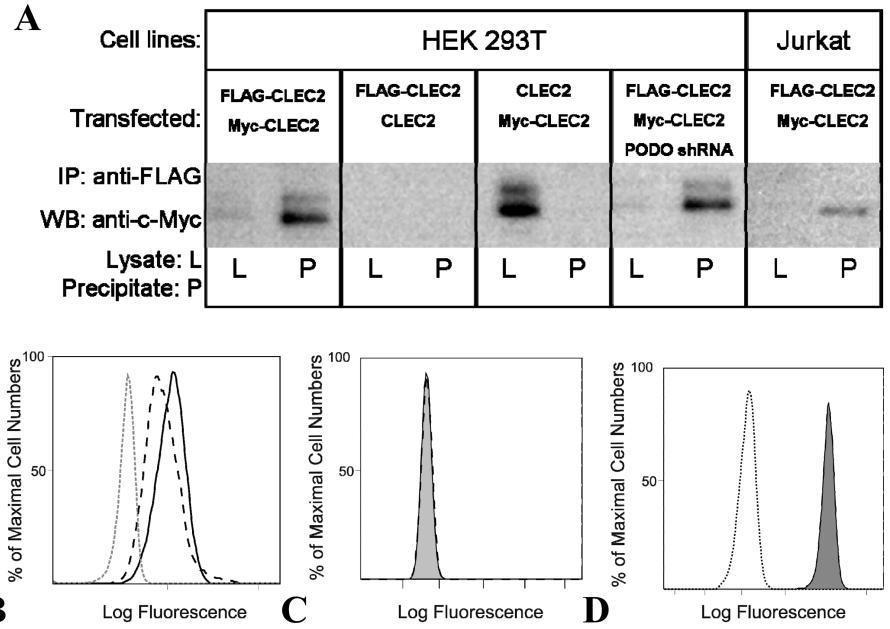

FIGURE 3: CLEC-2 undergoes dimerization in HEK 293T and in Jurkat cells. (A) HEK 293T (left) or Jurkat (right) cells were cotransfected with combinations of FLAG-tagged, c-Myc-tagged, or untagged full-length CLEC2, and cell lysates were immunoprecipitated with anti-FLAG antibody. c-Myc-tagged CLEC-2 was detected by Western blotting with anti-c-Myc antibody. Where indicated, HEK 293T cells were also transfected with a plasmid encoding a podoplanin shRNA construct ("PODO shRNA"). Results are representative of three experiments. For each sample, precipitated protein is labeled (P), and cellular lysates are labeled (L). (B) Flow cytometry using the anti-human podoplanin antibody NZ-1 with untransfected HEK 293T cells (solid black line) or cells transfected with a pSUPER RNAi vector targeted to silence podoplanin (dashed black line). The dotted gray line is an isotype control antibody. (C) Flow cytometry showing staining of Jurkat cells with either phycoerythrin-labeled CLEC-2 (filled histogram) or a phycoerythrin-labeled control protein (dashed black line), demonstrating that there is no binding of CLEC-2 to these cells, confirming that they do not express a ligand for CLEC-2. (D) Positive control demonstrating that the phycoerythrin-labeled CLEC-2 used in (C) binds to cells expressing a ligand for CLEC-2. HEK 293T cells which express podoplanin were stained with phycoerythrin-labeled CLEC-2 (filled histogram) compared to a phycoerythrin-labeled control protein (dashed black line).

CLEC-2 ligand as they are not bound by fluorescence-labeled multimeric CLEC-2 (*8*). The absence of a ligand for CLEC-2 in Jurkat cells was confirmed by flow cytometry using fluorescence-labeled multimeric CLEC-2 prior to the experiments (Figure 3C), and the activity of this CLEC-2 tetramer was confirmed by its binding to HEK 293T cells which express podoplanin (Figure 3D). Using Jurkat cells, transfected c-Myc-tagged CLEC-2 was also found to coimmunoprecipitate with FLAG-tagged CLEC-2 (Figure 3A), confirming that full-length CLEC-2 is a dimer or higher order multimer in the absence of its endogenous ligand, podoplanin.

Bioluminescence Resonance Energy Transfer Studies Confirm That CLEC-2 Is a Dimer. Bioluminescence resonance energy transfer-based (BRET) assays, which determine the efficiency of resonance energy transfer ($BRET_{eff}$) between test proteins fused with luciferase (i.e., donor) and GFP (i.e., acceptor), are useful for determining whether proteins oligomerize *in situ* in a largely nonperturbative manner. The transfer of energy between luciferase and GFP is highly dependent on the separation of the two fluorophores and falls to zero for separation distances of 10 nm or greater. Randomly interacting proteins give much weaker $BRET_{eff}$ levels than oligomers because their average separation distance is generally much larger than that of the subunits of oligomers. In addition, the $BRET_{eff}$ level for randomly interacting proteins, in contrast to that for oligomers, exhibits independence from the acceptor/donor ratio under conditions in which the acceptor level is kept essentially constant, as predicted by theory (discussed in ref *29*). Together, these two criteria can be used to distinguish between dimers and monomers.

HEK 293T cells were transiently cotransfected with plasmids expressing GFP2- and luciferase-tagged full-length CLEC-2 as a "BRET pair" (*29*). Surface expression of these constructs was confirmed by confocal microscopy and flow cytometric analysis of HEK 293T cells transfected with either GFP2- or luciferase-tagged full-length CLEC-2 (Figure 4 and data not shown). The dependence of $BRET_{eff}$ on the acceptor/donor ratio indicates that CLEC-2 is oligomeric; the fit of the data is consistent with CLEC-2 being a dimer (Figure 5). The $BRET_{eff}$ maximum for the CLEC-2 BRET pair lies between that determined for a known monomer, CD86 (Figure 5), and that for a disulfide-linked homodimer, CTLA-4 (*29*). The results are similar to those obtained previously for the nonconstitutive homodimer CD80, suggesting that human CLEC-2 also forms nonconstitutive homodimers at the cell surface (*29*). As far as we are aware, this is the first reported BRET analysis of type 2 membrane proteins.

CLEC-2 Does Not Form Disulfide-Linked Homodimers. To assess whether cysteines 81 and 99 within the stalk portion of CLEC-2 are involved in intra- or intermolecular disulfide bond formation, HEK 293T cells were transfected with a construct encoding either untagged full-length human CLEC-2 or GFP2-CLEC-2. The transfected cells were lysed and the lysates separated by SDS−PAGE under reducing or nonreducing conditions. Separated lysates were transferred onto nitrocellulose and blotted with monoclonal anti-CLEC-2 antibody, anti-GFP antibody, polyclonal anti-CLEC-2, or control Ig. In both reducing and nonreducing conditions only one major band was seen, which corresponded to monomeric CLEC2 protein (Figure 6). This is consistent with the mass spectrometry data and confirms that the additional extracellular cysteine residues present in the stalk region of CLEC-2 do not form intermolecular disulfide bridges between CLEC-2 monomers. The experiment was repeated using CLEC-2 that was tagged on its N-terminus with GFP2 (Figure 6). Similar results were obtained, confirming that the tagged proteins used in the BRET experiments behave in the same way as untagged protein.

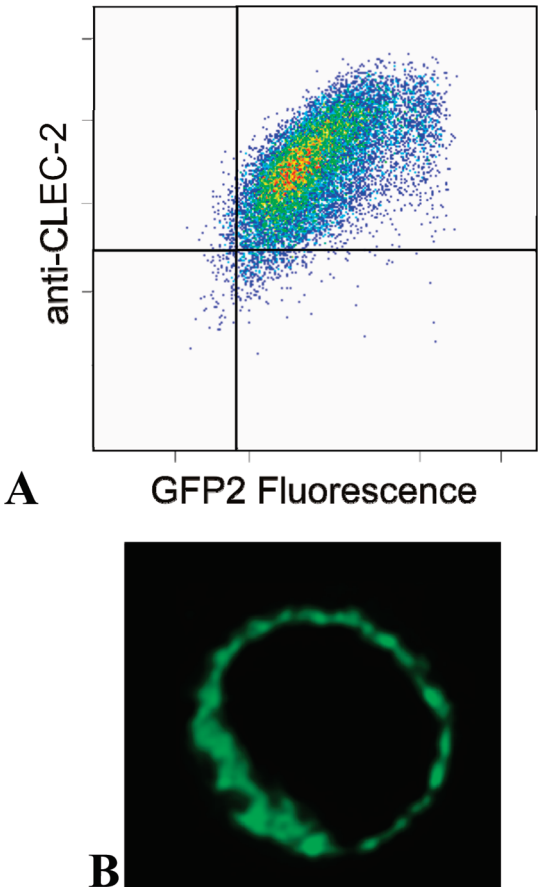

FIGURE 4: GFP2-tagged CLEC-2 is expressed on the surface of transfected HEK 293T cells. Nonpermeabilized HEK 293T cells were transfected with full-length CLEC-2 tagged with codon humanized GFP2 on its N-terminus and analyzed by flow cytometry for CLEC-2 expression using a monoclonal antibody against CLEC-2 (A) and by confocal microscopy (B). In (A), the *x*-axis represents GFP2 emission and so fusion protein expression, and the *y*-axis represents staining with the anti-CLEC-2 antibody, and surface expression of CLEC-2 is proportional to GFP expression.

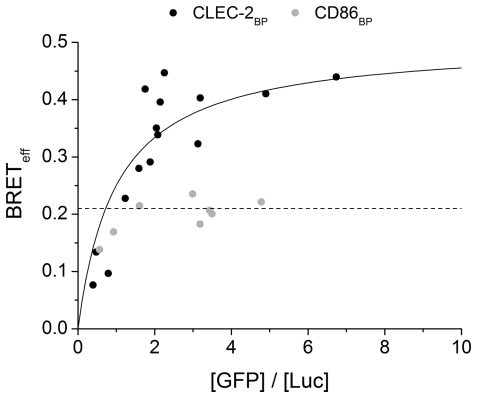

FIGURE 5: CLEC-2 dimerization as assessed by BRET analysis. HEK 293T cells were cotransfected with the GFP2-CLEC2/luciferase-CLEC2 pair (black dots) or the monomeric control pair CD86-GFP2 plus CD86-luciferase (gray dots) at varying DNA concentration ratios. The $BRET_{eff}$ trace for the CLEC-2 BRET pair is consistent with that of a non-disulfide-linked dimer, as compared to the $BRET_{eff}$ trace for monomeric CD86.

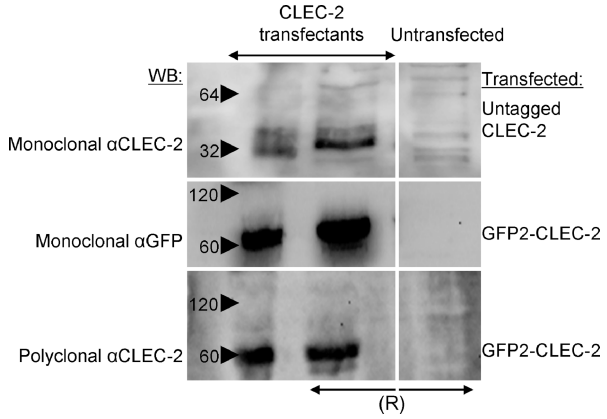

FIGURE 6: Full-length CLEC-2 is not a disulfide-linked homodimer in cells. HEK 293T cells were transfected with either (top panel) untagged CLEC-2 (32 kDa) or (middle and bottom panels) GFP2-CLEC-2 (60 kDa). Protein samples were separated on 15% SDS−PAGE gels, transferred, and Western blotted with 10 μg of either mouse monoclonal CLEC-2 antibody (top panel), mouse monoclonal anti-GFP antibody (middle panel), or polyclonal mouse anti-CLEC-2 (bottom panel). Samples loaded in reducing loading dye are indicated by "R". Approximate molecular masses (kDa) are indicated by black arrows on the left-hand side of each gel.

The Potential Flexibility of Dimeric CLEC-2 May Influence Ligand Binding. To explore the potential functional implications of the CLEC-2 structure, we have previously generated a structural model of dimeric CLEC-2 (*11*). We have now further refined this model in the light of the current data showing that CLEC-2 can form a non-disulfide linked homodimer (Figure 7A). Relative to its monomeric counterpart, dimeric CLEC-2 has a larger binding surface available, with a secondary set of charged residues within and around each long loop region and surrounding nonpolar patches, which could make hydrophobic interactions with a ligand. The dimer interface in the model includes hydrophobic interactions between phenylalanines at positions 116 and 117 and tyrosines at positions 109 and 148. However, these interacting forces are likely to be insufficient to maintain CLEC-2 in a dimeric form, as experimental data demonstrate that the stalk region is required for dimer formation (Figure 1). The stalk region is not included in the model as it does not have a clearly predictable secondary structure. The dynamic consequences of homodimerization on the ability of CLEC-2 to interact with a binding partner have not previously been studied. Therefore, we undertook molecular dynamics studies to examine the likely modes of motion of dimeric CLEC-2. A porcupine plot illustrates the results, showing the predicted capacity for the modeled dimer of CLEC-2 to move in a bimodal pattern, whereby the individual C-type lectin-like domain subunits "twist" relative to one another in an anticorrelated fashion (Figure 7B,C). This opposing directionality of the motions of each subunit may allow added flexibility within the ligand binding site, thus permitting it to better fit its ligands.

Rhodocytin Exists in a Range of Multimeric States Which May Further Cluster Dimeric CLEC-2 on the Platelet Surface. We have shown that rhodocytin, the snake venom ligand for CLEC-2, forms a non-disulfide-linked $(\alpha\beta)_2$ tetramer (*11*). This is the first example of a snake venom or other C-type lectin-like protein multimerizing in this way (*7*). While both convulxin and flavocetin-A $\alpha\beta$-heterodimers further multimerize to form cyclic $(\alpha\beta)_4$ complexes, these are covalently linked by interchain disulfide bonds (*37*, *38*). To probe whether the

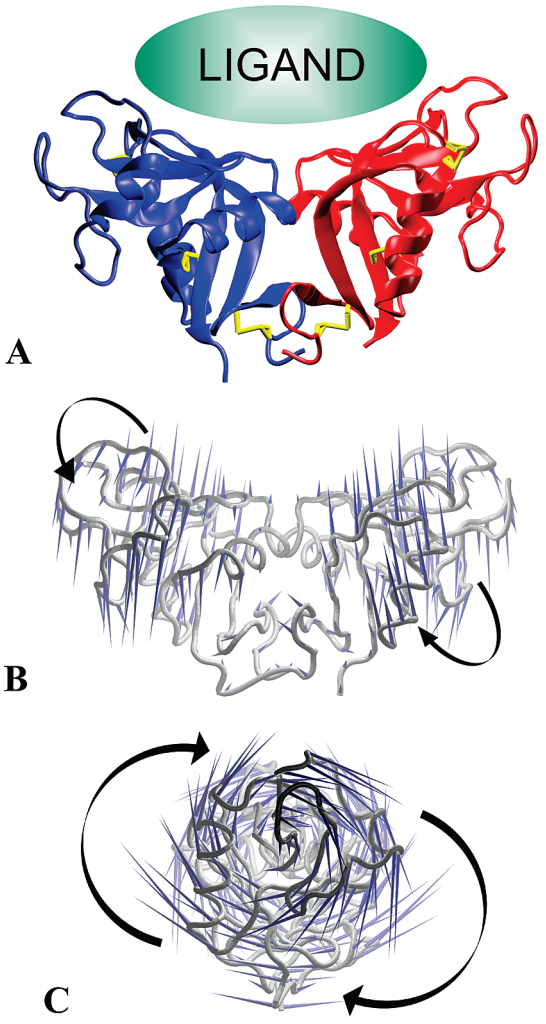

FIGURE 7: Model dimeric CLEC-2 is flexible, and this may enhance ligand binding. Molecular dynamics analysis of a model of dimeric CLEC-2. (A) Model dimeric CLEC-2 is represented as a cartoon where the individual monomer chains are colored blue and red. Disulfide bonds formed between cysteine residues are marked in yellow, and the putative ligand binding site is represented by a green oval. (B, C) Porcupine plots of the principal mode of conformational variability of the Cα atoms calculated from a CONCOORD ensemble are presented with each blue cone indicating the direction of motion of the atom and the lengths indicating the relative amplitude of the motion. Panel C is related to panel B by a 90° clockwise rotation about the *y*-axis. Black arrows indicate opposing motions of the two C-type lectin-like domains, demonstrating how the bimodal pattern of motion may allow spreading of the ligand binding region to enhance the ligand interaction.

noncovalent nature of the assembly of the rhodocytin tetramer allows the formation of higher order multimeric complexes of rhodocytin, size exclusion chromatography of rhodocytin with online multiangle laser light scattering (MALS) was employed. The MALS data demonstrate that rhodocytin is polydisperse in terms of its molecular mass, existing principally as an $(\alpha\beta)_2$-tetramer, but notably also as a higher order multimeric assembly. Three peaks are observed in the size exclusion chromatography trace (Figure 8). The first peak includes a broad range of masses decreasing from > 150 to 70 kDa (Figure 8). The pattern in which the mass declines across this peak suggests that this peak may represent two or more 60−70 kDa species in a dynamic equilibrium. The second peak is monodisperse and represents a species of mass ~68−73 kDa, consistent with tetrameric rhodocytin (Figure 8). The third peak corresponds to an ~37 kDa form of

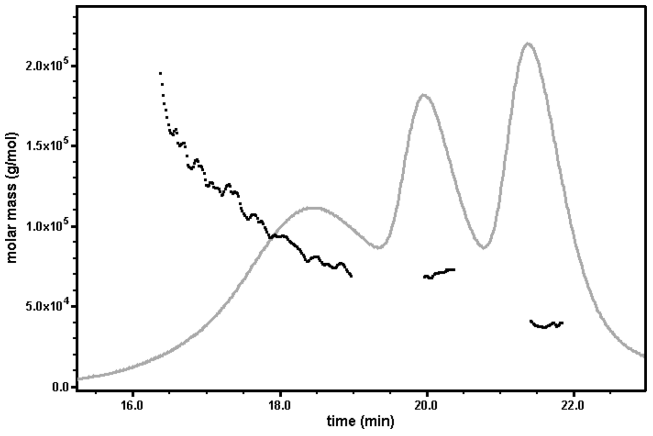

FIGURE 8: Rhodocytin can adopt a range of multimeric states in solution. MALS experiments using an analytical Superdex S75 10/30 gel filtration column with online static light scattering, differential refractive index, and UV detectors. Data were analyzed using the ASTRA software package (Wyatt Technology). The sample refractive index and molar mass are represented as gray and black traces, respectively, with elution time plotted on the *x*-axis.

rhodocytin (Figure 8), which suggests that rhodocytin may also exist as $\alpha\beta$-heterodimeric subunits in solution. Given the breadth and polydispersity of the initial 150−70 kDa peak, these MALS-defined molecular size estimations for the $\alpha\beta$-heterodimer and $(\alpha\beta)_2$-tetramer are consistent with previously reported masses determined by mass spectrometry and SDS−PAGE (*26*).

DISCUSSION

We have studied the oligomerization of CLEC-2, as this is relevant to an understanding of its ligand binding properties and of its ability to signal through spleen tyrosine kinase Syk, despite having only a single YXXL signaling motif in its cytoplasmic tail (*7*, *15*). Bacterial protein lacking the stalk region is exclusively monomeric (*10*, *12*). However, protein expressed in *E. coli* from construct pOC550, which encodes the stalk region N-terminal to the crystallographically determined C-type lectin-like domain (Figure 1), was shown by gel filtration size exclusion chromatography to exist as both a homodimer and a monomer (Figure 1C). Furthermore, CLEC-2 protein identical in sequence to pOC550, but produced in a mammalian expression system, is exclusively dimeric (Figure 1D). As the bacterial protein is not glycosylated, this suggests that glycosylation plays a role in stabilizing the dimer, possibly through an effect on the stalk region. There is a predicted N-terminal glycosylation site at position 68 within the stalk region which may also be important for dimerization. The absence of the monomeric form in protein produced in eukaryotic cells certainly suggests the influence of additional effects on dimer formation, possibly from glycosylation, eukaryotic protein folding chaperone activity, or degradation of misfolded protein. The putative stalk region has no predicted secondary structure, and comparison with other C-type lectin-like molecules does not demonstrate any evidence of a conserved role for this domain in lectin oligomerization. The influence of the stalk region suggests that it may stabilize the otherwise weak interactions between the predicted "dimerization patches" on two CLEC-2 monomers (*10*). Dimeric protein was functional in surface plasmon resonance binding studies and appears to have a higher affinity than monomeric protein (*8*).

Several related members of the C-type lectin-like family of proteins, including NKG2D, LOX-1, and CD69, and the mouse Ly49 family of immunoreceptors, exist as disulfide-linked homodimers (*23*, *24*, *39*, *40*). However, the two additional extracellular cysteine residues present in the stalk region of CLEC-2 do not form interchain disulfide bridges between CLEC-2 monomers (Figure 6) and probably form an intrachain disulfide bond as occurs in the related C-type lectin-like molecule CD94 (*41*). Coimmunoprecipitation of CLEC-2 demonstrates that CLEC-2 is multimeric, as FLAG-tagged CLEC-2 is able to coimmunoprecipitate myc-tagged CLEC-2 (Figure 3). Quantitative BRET studies show that CLEC-2 can homodimerize noncovalently in HEK 293T cells (Figure 4). This interaction is independent of the presence of the CLEC-2 ligand, podoplanin, as CLEC-2 is self-associating in HEK 293T cells in which podoplanin expression was reduced using RNAi and in Jurkat cells which do not express a ligand for CLEC-2 (Figure 3).

Dimeric CLEC-2 may allow more flexible ligand binding than monomeric CLEC-2 (Figure 7). The potential bimodal movements of the two C-type lectin-like domains relative to one another may enable the dimeric CLEC-2 binding site to accommodate both of its structurally diverse ligands, rhodocytin and podoplanin. For soluble and membrane-bound ligands which bind surface receptors on platelets with intracellular cytoplasmic signaling elements, the capacity to cluster the receptor may be highly advantageous (*37*, *38*). The multiangle light scattering data presented demonstrate that rhodocytin exists in solution in a number of different forms, with the dominant species being an $(\alpha\beta)_2$-tetramer, which may further oligomerize in a range of multimeric conformations (Figure 8). This polydispersity is consistent with rhodocytin being in a dynamic equilibrium between these alternative conformations in solution. The existence of larger multimeric assemblies of rhodocytin suggests that it can present several equivalent concave binding surfaces to engage and cluster dimeric CLEC-2 receptors on the platelet surface (*11*). Ligand binding may stabilize one or more of these states. Higher order multimericity in the related snake venoms convulxin and flavocetin-A is believed to promote clustering of the cognate receptor on the platelet surface (GPVI for convulxin and GPIb for flavocetin-A), thus augmenting signal transduction activity (*37*, *38*).

Dimerization of CLEC-2 and possible further ligand-induced clustering could be important in signaling with only a single YXXL motif rather than a full ITAM. The propensity for CLEC-2 dimerization at the cell surface raises the possibility that one Syk molecule could interact with two CLEC-2 monomers and so with two YXXL motifs.

ACKNOWLEDGMENT

Christopher Pugh kindly provided us with plasmids which we used to create our BRET constructs. Rhodocytin was a gift from Johannes Eble, and CD44 was a gift from David Jackson. We thank Steve Watson, Kate Wicks, Geoff Sutton, Benjamin Hall, and Matthew Cockman for useful advice and discussions.

REFERENCES

1. Mackman, N. (2008) Triggers, targets and treatments for thrombosis. *Nature 451*, 914–918.
2. George, J. N. (2000) Platelets. *Lancet 355*, 1531–1539.
3. Meadows, T. A., and Bhatt, D. L. (2007) Clinical aspects of platelet inhibitors and thrombus formation. *Circ. Res. 100*, 1261–1275.
4. Colonna, M., Samaridis, J., and Angman, L. (2000) Molecular characterization of two novel C-type lectin-like receptors, one of which is selectively expressed in human dendritic cells. *Eur. J. Immunol. 30*, 697–704.

5. Sobanov, Y., Bernreiter, A., Derdak, S., Mechtcheriakova, D., Schweighofer, B., Duchler, M., Kalthoff, F., and Hofer, E. (2001) A novel cluster of lectin-like receptor genes expressed in monocytic, dendritic and endothelial cells maps close to the NK receptor genes in the human NK gene complex. *Eur. J. Immunol. 31*, 3493–3503.
6. Sawamura, T., Kume, N., Aoyama, T., Moriwaki, H., Hoshikawa, H., Aiba, Y., Tanaka, T., Miwa, S., Katsura, Y., Kita, T., and Masaki, T. (1997) An endothelial receptor for oxidized low-density lipoprotein. *Nature 386*, 73–77.
7. Suzuki-Inoue, K., Fuller, G. L., Garcia, A., Eble, J. A., Pohlmann, S., Inoue, O., Gartner, T. K., Hughan, S. C., Pearce, A. C., Laing, G. D., Theakston, R. D., Schweighoffer, E., Zitzmann, N., Morita, T., Tybulewicz, V. L., Ozaki, Y., and Watson, S. P. (2006) A novel Syk-dependent mechanism of platelet activation by the C-type lectin receptor CLEC-2. *Blood 107*, 542–549.
8. Christou, C. M., Pearce, A. C., Watson, A. A., Mistry, A. R., Pollitt, A. Y., Fenton-May, A. E., Johnson, L. A., Jackson, D. G., Watson, S. P., and O'Callaghan, C. A. (2008) Renal cells activate the platelet receptor CLEC-2 through podoplanin. *Biochem. J. 411*, 133–140.
9. Suzuki-Inoue, K., Kato, Y., Inoue, O., Kaneko, M. K., Mishima, K., Yatomi, Y., Yamazaki, Y., Narimatsu, H., and Ozaki, Y. (2007) Involvement of the snake toxin receptor CLEC-2, in podoplanin-mediated platelet activation, by cancer cells. *J. Biol. Chem. 282*, 25993–26001.
10. Watson, A. A., Brown, J., Harlos, K., Eble, J. A., Walter, T. S., and O'Callaghan, C. A. (2007) The crystal structure and mutational binding analysis of the extracellular domain of the platelet-activating receptor CLEC-2. *J. Biol. Chem. 282*, 3165–3172.
11. Watson, A. A., Eble, J. A., and O'Callaghan, C. A. (2008) Crystal structure of rhodocytin, a ligand for the platelet-activating receptor CLEC-2. *Protein Sci. 17*, 1611–1616.
12. Watson, A. A., and O'Callaghan, C. A. (2005) Crystallization and X-ray diffraction analysis of human CLEC-2. *Acta Crystallogr., Sect. F: Struct. Biol. Cryst. Commun. 61*, 1094–1096.
13. O'Callaghan, C. A. (2009) Thrombomodulation via CLEC-2 targeting. *Curr. Opin. Pharmacol. 9*, 90–95.
14. Suzuki-Inoue, K., Kato, Y., Inoue, O., Kaneko, M. K., Mishima, K., Yatomi, Y., Narimatsu, H., and Ozaki, Y. (2007) Involvement of the snake toxin receptor CLEC-2 in podoplanin-mediated platelet activation by cancer cells. *J. Biol. Chem. 282*, 25993–26001.
15. Fuller, G. L., Williams, J. A., Tomlinson, M. G., Eble, J. A., Hanna, S. L., Pohlmann, S., Suzuki-Inoue, K., Ozaki, Y., Watson, S. P., and Pearce, A. C. (2007) The C-type lectin receptors CLEC-2 and Dectin-1, but not DC-SIGN, signal via a novel YXXL-dependent signaling cascade. *J. Biol. Chem. 282*, 12397–12409.
16. Ivashkiv, L. B. (2009) Cross-regulation of signaling by ITAM-associated receptors. *Nat. Immunol. 10*, 340–347.
17. Iwashima, M., Irving, B. A., van Oers, N. S., Chan, A. C., and Weiss, A. (1994) Sequential interactions of the TCR with two distinct cytoplasmic tyrosine kinases. *Science 263*, 1136–1139.
18. Koyasu, S., Tse, A. G., Moingeon, P., Hussey, R. E., Mildonian, A., Hannisian, J., Clayton, L. K., and Reinherz, E. L. (1994) Delineation of a T-cell activation motif required for binding of protein tyrosine kinases containing tandem SH2 domains. *Proc. Natl. Acad. Sci. U.S.A. 91*, 6693–6697.
19. Pao, L. I., Famiglietti, S. J., and Cambier, J. C. (1998) Asymmetrical phosphorylation and function of immunoreceptor tyrosine-based activation motif tyrosines in B cell antigen receptor signal transduction. *J. Immunol. 160*, 3305–3314.
20. Rowley, R. B., Burkhardt, A. L., Chao, H. G., Matsueda, G. R., and Bolen, J. B. (1995) Syk protein-tyrosine kinase is regulated by tyrosine-phosphorylated Ig alpha/Ig beta immunoreceptor tyrosine activation motif binding and autophosphorylation. *J. Biol. Chem. 270*, 11590–11594.
21. Ohki, I., Ishigaki, T., Oyama, T., Matsunaga, S., Xie, Q., Ohnishi-Kameyama, M., Murata, T., Tsuchiya, D., Machida, S., Morikawa, K., and Tate, S. (2005) Crystal structure of human lectin-like, oxidized low-density lipoprotein receptor 1 ligand binding domain and its ligand recognition mode to OxLDL. *Structure* (*Cambridge*) *13*, 905–917.
22. Radaev, S., Rostro, B., Brooks, A. G., Colonna, M., and Sun, P. D. (2001) Conformational plasticity revealed by the cocrystal structure of NKG2D and its class I MHC-like ligand ULBP3. *Immunity 15*, 1039–1049.
23. Dam, J., Guan, R., Natarajan, K., Dimasi, N., Chlewicki, L. K., Kranz, D. M., Schuck, P., Margulies, D. H., and Mariuzza, R. A. (2003) Variable MHC class I engagement by Ly49 natural killer cell receptors demonstrated by the crystal structure of Ly49C bound to H-2K(b). *Nat. Immunol. 4*, 1213–1222.
24. Natarajan, K., Sawicki, M. W., Margulies, D. H., and Mariuzza, R. A. (2000) Crystal structure of human CD69: a C-type lectin-like activation marker of hematopoietic cells. *Biochemistry 39*, 14779–14786.
25. Park, H., Adsit, F. G., and Boyington, J. C. (2005) The 1.4 angstrom crystal structure of the human oxidized low density lipoprotein receptor lox-1. *J. Biol. Chem. 280*, 13593–13599.
26. Watson, A. A., and O'Callaghan, C. A. (2005) Crystallization and X-ray diffraction analysis of human CLEC-2. *Acta Crystallogr., Sect. F: Struct. Biol. Cryst. Commun. 61*, 1094–10096.
27. Bergmeier, W., Bouvard, D., Eble, J. A., Mokhtari-Nejad, R., Schulte, V., Zirngibl, H., Brakebusch, C., Fassler, R., and Nieswandt, B. (2001) Rhodocytin (aggretin) activates platelets lacking alpha(2)beta(1) integrin, glycoprotein VI, and the ligand-binding domain of glycoprotein Ibalpha. *J. Biol. Chem. 276*, 25121–25126.
28. Eble, J. A., Beermann, B., Hinz, H. J., and Schmidt-Hederich, A. (2001) alpha 2beta 1 integrin is not recognized by rhodocytin but is the specific, high affinity target of rhodocetin, an RGD-independent disintegrin and potent inhibitor of cell adhesion to collagen. *J. Biol. Chem. 276*, 12274–12284.
29. James, J. R., Oliveira, M. I., Carmo, A. M., Iaboni, A., and Davis, S. J. (2006) A rigorous experimental framework for detecting protein oligomerization using bioluminescence resonance energy transfer. *Nat. Methods 3*, 1001–1006.
30. O'Callaghan, C. A., Cerwenka, A., Willcox, B. E., Lanier, L. L., and Bjorkman, P. J. (2001) Molecular competition for NKG2D: H60 and RAE1 compete unequally for NKG2D with dominance of H60. *Immunity 15*, 201–211.
31. Emsley, P., and Cowtan, K. (2004) Coot: model-building tools for molecular graphics. *Acta Crystallogr., Sect. D: Biol. Crystallogr. 60*, 2126–2132.
32. Vriend, G. (1990) WHAT IF: A molecular modeling and drug design program. *J. Mol. Graphics 8*, 52–56.
33. Brunger, A. T., Adams, P. D., Clore, G. M., DeLano, W. L., Gros, P., Grosse-Kunstleve, R. W., Jiang, J. S., Kuszewski, J., Nilges, M., Pannu, N. S., Read, R. J., Rice, L. M., Simonson, T., and Warren, G. L. (1998) Crystallography & NMR system: A new software suite for macromolecular structure determination. *Acta Crystallogr., Sect. D: Biol. Crystallogr. 54* (Part 5), 905–921.
34. Barrett, C. P., Hall, B. A., and Noble, M. E. (2004) Dynamite: a simple way to gain insight into protein motions. *Acta Crystallogr., Sect. D: Biol. Crystallogr. 60*, 2280–2287.
35. Humphrey, W., Dalke, A., and Schulten, K. (1996) VMD: visual molecular dynamics. *J. Mol. Graphics 14*, 27–28.
36. Schacht, V., Dadras, S. S., Johnson, L. A., Jackson, D. G., Hong, Y. K., and Detmar, M. (2005) Up-regulation of the lymphatic marker podoplanin, a mucin-type transmembrane glycoprotein, in human squamous cell carcinomas and germ cell tumors. *Am. J. Pathol. 166*, 913–921.
37. Batuwangala, T., Leduc, M., Gibbins, J. M., Bon, C., and Jones, E. Y. (2004) Structure of the snake-venom toxin convulxin. *Acta Crystallogr., Sect. D: Biol. Crystallogr. 60*, 46–53.
38. Fukuda, K., Mizuno, H., Atoda, H., and Morita, T. (2000) Crystal structure of flavocetin-A, a platelet glycoprotein Ib-binding protein, reveals a novel cyclic tetramer of C-type lectin-like heterodimers. *Biochemistry 39*, 1915–1923.
39. Ohki, I., Ishigaki, T., Oyama, T., Matsunaga, S., Xie, Q., Ohnishi-Kameyama, M., Murata, T., Tsuchiya, D., Machida, S., Morikawa, K., and Tate, S. (2005) Crystal structure of human lectin-like, oxidized low-density lipoprotein receptor 1 ligand binding domain and its ligand recognition mode to OxLDL. *Structure 13*, 905–917.
40. Wu, J., Song, Y., Bakker, A. B., Bauer, S., Spies, T., Lanier, L. L., and Phillips, J. H. (1999) An activating immunoreceptor complex formed by NKG2D and DAP10. *Science 285*, 730–732.
41. Boyington, J. C., Riaz, A. N., Patamawenu, A., Coligan, J. E., Brooks, A. G., and Sun, P. D. (1999) Structure of CD94 reveals a novel C-type lectin fold: implications for the NK cell-associated CD94/NKG2 receptors. *Immunity 10*, 75–82.